32ND INTERNATIONAL COSMIC RAY CONFERENCE, BEIJING 2011


# The search for extremely high-energy neutrinos with IceCube

THE ICECUBE COLLABORATION[1]
[1]*See special section in these proceedings*

**Abstract:** The IceCube neutrino telescope was constructed to search for high energy neutrinos of cosmic origin. At the highest energies, neutrinos associated with the interaction of the most energetic cosmic rays with cosmic microwave background photons (GZK effect) are considered a guaranteed signal, with expected event rates of up to a few events per year in a cubic kilometer detector. Searches for GZK neutrinos have been performed using data taken with the intermediate construction stages of the now complete IceCube detector. We present the results of finished and on-going analyses, with a focus on the search using data taken between spring 2009 and spring 2010, when the IceCube detector was roughly 70% complete.

**Corresponding authors:** Henrike Wissing[2] *(hwissing@icecube.umd.edu)*, Aya Ishihara[3] *(aya@hepburn.s.chiba-u.ac.jp)*
[2] *University of Maryland. College Park, MD 20742, USA*
[3] *Chiba University, Chiba 263-8522, Japan*

DOI: 10.7529/ICRC2011/V02/0949

**Keywords:** IceCube, GZK neutrinos, EHE neurtinos

## 1 Introduction

The detection of extremely-high energy (EHE) neutrinos with energies in excess of $10^7$ GeV may shed light on the yet unknown origin of the highest energy cosmic rays. The direct observation of EHE charged cosmic ray particles is limited by their inevitable energy loss in the cosmic microwave background through photo-pion production, known as the Greisen-Zatsepin-Kuzmin (GZK) effect [1]. The trajectories of the charged cosmic ray particles with diminished energies will have been randomized in cosmic magnetic fields upon arrival at the Earth. Neutrinos from the decays of the secondary charged pions, $\pi^{\pm} \rightarrow \mu^{\pm}\nu_{\mu} \rightarrow e^{\pm}\nu_e\nu_{\mu}\nu_{\mu}$, will travel in straight lines and unattenuated over cosmological distances and carry information about the sources of EHE cosmic rays.

The IceCube neutrino observatory consists of a cubic kilometer sized Cherenkov detector embedded in the 2800 m thick glacial ice cap at the South Pole and an overlying square kilometer surface air-shower array. The in-ice detector consists of 5160 light sensitive digital optical modules (DOMs) deployed at depths between 1450 and 2450 m on 86 vertical cables ("strings"). Each DOM is equipped with a 25 cm photo-multiplier tube (PMT) along with two waveform digitizers and supporting data acquisition, calibration, and control hardware [2, 3]. Interactions of high energy neutrinos with the surrounding matter are detected via their Cherenkov emissions in the highly transparent Polar ice [4]. With its large detection volume, the in-ice detector is the first neutrino telescope with a realistic chance to detect the small flux of EHE neutrinos associated with the GZK effect.

During IceCube's construction phase, which started in 2005, data taken with the partially instrumented in-ice neutrino telescope have been searched for signatures of EHE neutrinos [5, 6]. The analysis of data taken during the years 2008/2009, when 40 of the 86 strings of the in-ice detector were deployed, has led to the currently most stringent limits on fluxes of EHE neutrinos with energies between 1 PeV and 10 EeV (Figure 1). In these proceedings, we report on a search for EHE neutrinos in data taken with the 59-string detector between spring 2009 and spring 2010.

## 2 Method

The vast majority of the events recorded by IceCube are due to down-going atmospheric muons that are created by interactions of high energy cosmic rays in the atmosphere, and which are sufficiently energetic to penetrate the ice overburden and deposit Cherenkov light in the detector. Against this background, an EHE neutrino interaction inside or in the vicinity of the detector would stand out with a much higher Cherenkov light deposition. Figure 2 shows the expected light deposition in terms of the number of recorded photo-electrons ($NPE$) and its correlation with the zenith angle ($\cos\Theta$) of the primary particle tracks for simulated GZK neutrino induced events and simulated at-

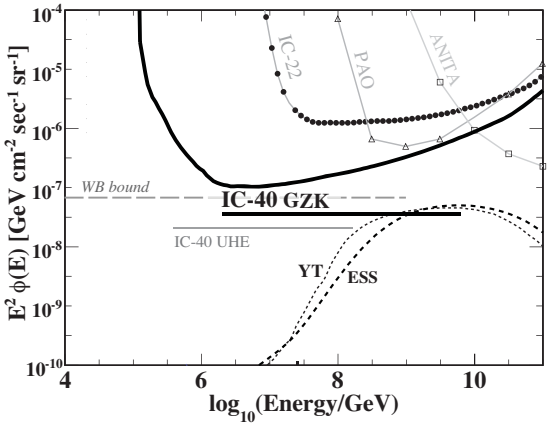


Figure 1: Present flux limits on EHE neutrinos compared to two all flavor GZK neutrino flux predictions, YT ((m, $Z_{max}$) = (4,4) [7] and ESS ($\Omega_\Lambda$ = 0.7) [8], and the Waxman-Bahcall bound [9]. Limits from IceCube 40-string GZK neutrino search (IC-40 GZK, differential limit and $E^{-2}$ spectrum integrated limit) [6] are shown as thick black lines, the limit from an UHE neutrino search (IC-40 UHE) [10] is shown as grey horizontal line. Less stringent limits were set by Auger (PAO) [11], ANITA [12], and the IceCube 22-string detector (IC-22) [5].

mospheric background events. For both signal and background events, the light yield is strongly correlated with $\cos\Theta$. For down-going atmospheric muon events, the expected $NPE$ rapidly decreases with increasing inclination of primary particle track, because with increasing slant depth the muons will lose more energy before reaching the detector. Below the horizon ($\cos\Theta < 0$), low energy atmospheric neutrinos arriving from the opposite hemisphere are the only expected background. The detection probability of GZK neutrinos is highest for directions close to the horizon, because of the relatively short neutrino interaction length at EHE energies.

Exploiting the correlation between the event light yield and the track direction, the data selection criteria to separate signal from background events in IceCube's EHE neutrino searches have routinely been designed as two-dimensional boundaries in the $NPE$-$\cos\Theta$-plane [5, 6]. Simple geometric fit methods, whose performance proved robust against systematic uncertainties in the detector response, were used to infer the track directions. In this analysis, we follow the same strategy, but we use a different fitting algorithm than previous analyses to determine the track direction.

Following a blind analysis procedure, the selection criteria are optimized on simulated signal and background events. A subset of 10% of the experimental data, evenly distributed throughout the data taking period, is used to validate the detector simulation. After the selection criteria are developed, the data selection is applied to the blinded 90% of the data, which for the 2009/2010 data-taking period roughly comprises 330 days of detector livetime. The 10% subset is discarded, in order to avoid statistical bias.

## 3 Monte Carlo simulations

The dominant background at the final data selection levels is high multiplicity muon bundles induced predominantly by heavy cosmic ray primaries with PeV to EeV energies. This background was simulated with the CORSIKA air-shower simulation [13] using the SIBYLL 2.1 [14] hadronic interaction model. Two primary types, proton and iron, with energies between $10^4$ and $10^{11}$ GeV were simulated. The primaries were sampled from a power-law energy spectrum following $dN/dE \propto E^{-2}$, in oder to over-sample the high energy end of the cosmic ray spectrum, which is most important to this analysis. Proton and iron components are then re-weighted to broken power-law spectra, whose combination approximates the all particle spectrum at PeV energies and above [15].

Signal events induced by EHE neutrinos in the energy range between $10^5$ and $10^{11}$ GeV were simulated with the JULIET package [16]. The charged secondary particles were sampled from an energy spectrum $\propto E^{-1}$. The events can be re-weighted to various GZK neutrino flux predictions. In these proceedings, we use the predictions from references [7] and [8] (*c. f.* YT and ESS in Figure 1). The quoted event rates correspond to the sum of all three neutrino flavors, $\nu_e$, $\nu_\mu$, and $\nu_\tau$.

## 4 Event selection

The first data selection for the various IceCube analyses is performed on-line at the South Pole, before data are sent to the northern hemisphere. For this analysis, the on-line filter required a minimum of 630 photo-electrons to be recorded in an event.

Following the analysis strategy that was developed for the 40-string detector [6], further data reduction is achieved by requiring at least 200 DOMs to have registered light within a time window of $[-4.4\mu s, 6.4\mu s]$ around the largest local light deposition in the detector. The latter is defined as the time at which 10% of the largest PMT pulse was captured. Further, we require the total number of photo-electrons recorded in this time window to be larger than 3200. With these requirements, the atmospheric background is reduced by two orders of magnitude, while 75% of the signal is retained (Table 1). While the previous EHE search used the *linefit* algorithm [17, 5] to reconstruct the track directions, we use a different algorithm in this analysis, the *dipolefit* [17]. The dipolefit assigns a dipole moment, $\vec{M}$, to the light pattern recorded in each event:

$$\vec{M} = \frac{1}{\frac{N_{\mathrm{DOM}}}{2}} \cdot \sum_{i=\frac{N_{\mathrm{DOM}}}{2}+1}^{N_{\mathrm{DOM}}} \frac{\vec{r}_i - \vec{r}_{i-\frac{N_{\mathrm{DOM}}}{2}}}{|\vec{r}_i - \vec{r}_{i-\frac{N_{\mathrm{DOM}}}{2}}|}, \qquad (1)$$

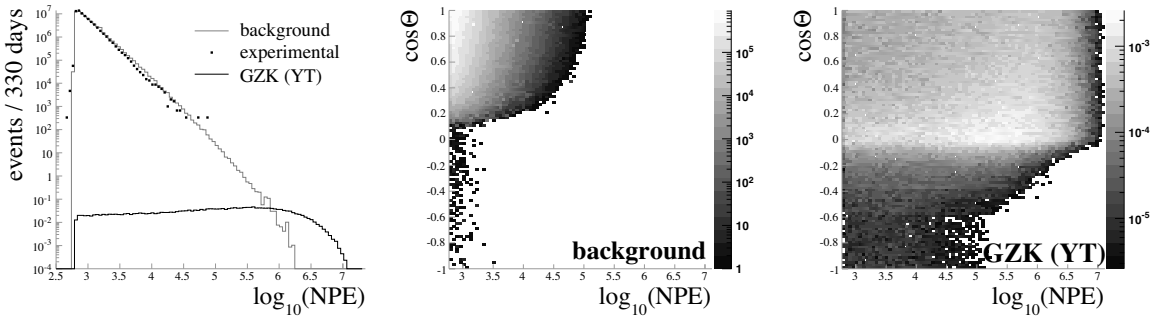


Figure 2: Expected light yield (logarithm of the number of detected photoelectrons, $\log_{10}(NPE)$), for simulated signal and background events and a subset of the experimental data set (left) and the correlation with the cosine of the zenith angle of the primary particle tracks for simulated atmospheric background events (middle) and GZK neutrinos (right). The background prediction includes cosmic ray induced muons, assuming a cosmic ray spectrum according to [15], and atmospheric neutrinos according to [18] with a contribution from prompt neutrinos according to [19]. The GZK neutrino spectrum is simulated according to [7] (*c. f.* YT in Figure 1).

| cut | Experimental | Background | GZK YT [7] | GZK ESS [8] |
|---|---|---|---|---|
| $NPE > 630$ | $6.20 \times 10^7$ | $(6.86 \pm 0.18) \times 10^7$ | $2.35 \pm 0.01$ | $1.81 \pm 0.01$ |
| $NPE > 3200$ and $N_{\mathrm{DOM}} > 200$ | $6.65 \times 10^5$ | $(7.68 \pm 0.12) \times 10^5$ | $1.80 \pm 0.01$ | $1.38 \pm 0.01$ |
| $\log_{10}(NPE) - 0.5 \cdot \mathcal{D} > 4$ | 336 | $365 \pm 6$ | $1.39 \pm 0.01$ | $1.07 \pm 0.01$ |

Table 1: Expected event rates at various selection levels for 330 days of detector livetime. The signal rates correspond to the GZK neutrino models according to [7] (YT) and [8] (ESS). Errors are statistical only.

where $\vec{r}_i$ is the vector of spatial coordinates of the DOM that recorded the $ith$ light signal in time, and $N_{\mathrm{DOM}}$ is the total number of DOMs fired in the event. The magnitude of the dipole moment $|\vec{M}|$ takes values between 0 and 1, and provides a measure for the directionality of the light flow in the event: large values of $|\vec{M}|$ indicate a track-like signal, while small values indicate a rather spherical light pattern. EHE neutrino interactions typically yield small dipole moments. Cascades induced by $\nu_e$ and $\nu_\tau$ interactions naturally generate spherical light patterns, and the light pattern from $\nu_\mu$ induced EHE muons has a broad radial distribution. Low energy atmospheric muon events on the other hand, typically have dipole moments close to 1.

Figure 3 shows the correlation between the magnitude and the direction ($\cos\Theta_{\mathrm{M}}$) of the dipole moment for atmospheric background events and GZK neutrino signal. Background events cluster in the region with large dipole moments and down-going directions. A combination of both magnitude and direction of the dipole moment, $\mathcal{D} = \cos\Theta_{\mathrm{M}} + 2 \cdot |\vec{M}|$, is used as a measure of the similarity of an event to a down-going track. Compared to a cut on the reconstructed direction only, a larger fraction of the extremely bright EHE neutrino signal events is preserved.

Background events with low values of $\mathcal{D}$ are predominantly induced by low energy neutrinos and atmospheric muons that pass outside the instrumented volume and deposit only very little Cherenkov light. Figure 4 shows the correlation of $\mathcal{D}$ with the light yield $NPE$. Signal and background events are well separated in the $\mathcal{D}$-$NPE$-plane. A two-dimensional cut in this plane defined by $(\log_{10}(NPE) - 0.5 \cdot \mathcal{D}) > 4$ reduces the atmospheric background by two more orders of magnitude, while the expected GZK neutrino signal still exceeds one event in 330 days (Table 1).

Additional selection criteria to separate the GZK signal events from the remaining background are being investigated. A realistic chance to detect a GZK neutrino signal requires the further selection criteria to keep the signal expectation above 1 event, while suppressing the background to a level of $\mathcal{O}(0.1)$ expected events per year. The GZK neutrino search with the 40-string detector [6] achieved a signal expectation of 0.5 events for GZK models presented here, above an expected background of roughly 0.1 events at the final selection level. With the larger 59-string detector, improved event selection criteria, and better understanding of the detector response, the required signal to background ratio to either detect GZK neutrinos or to constrain the here considered flux predictions seems within reach.

## 5 Conclusions

The detection of GZK neutrinos with IceCube seems tantalizingly close. The analysis of data taken with an intermediate construction stage of the detector, in which half the in-ice detector was deployed, allowed to place the most stringent limits on EHE neutrinos to-date. Data taken with later construction stages are presently being analyzed. Already the next construction stage, which roughly 70% of

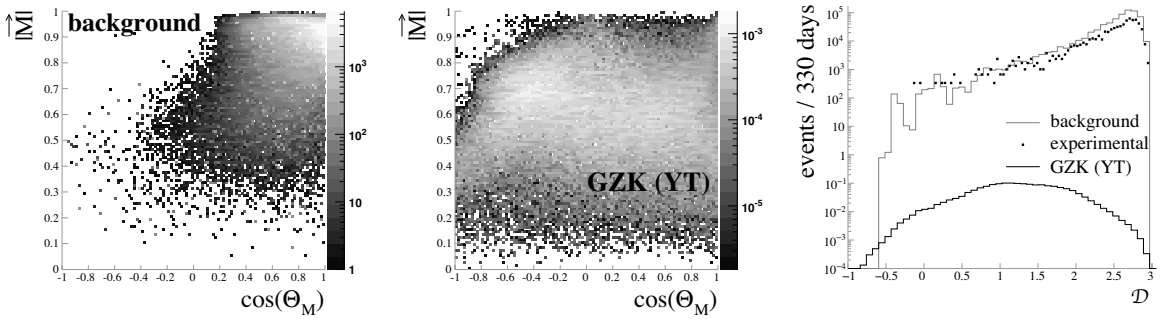


Figure 3: Observables of the *dipolefit*. The magnitude of the dipole moment $|\vec{M}|$ versus the reconstructed zenith angle ($\cos\Theta_{\mathrm{M}}$) for simulated background events (left) and simulated signal events (middle). The linear combination $\mathcal{D} = \cos\Theta_{\mathrm{M}} + 2 \cdot |\vec{M}|$ (right), is a measure the similarity of the event to a down-going track.

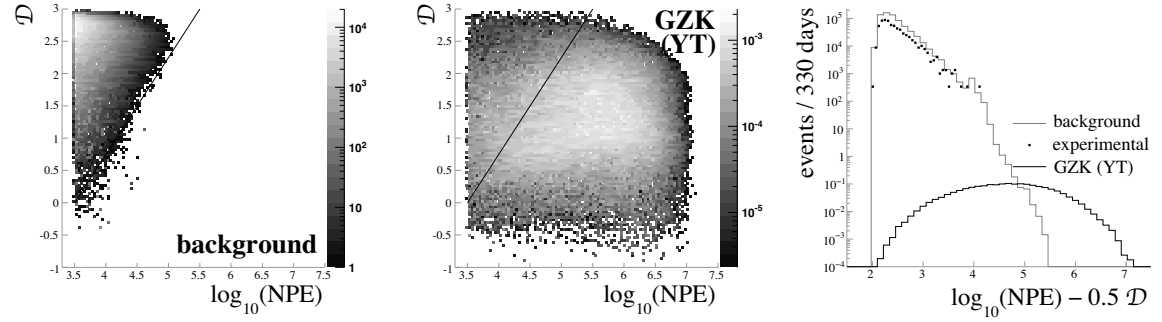


Figure 4: Correlation of the combined dipole observable $\mathcal{D} = \cos\Theta_{\mathrm{M}} + 2 \cdot |\vec{M}|$ with $NPE$ for simulated background events (left) and simulated signal events (middle). The linear combination of $\mathcal{D}$ and $NPE$ that is used as a cut parameter is shown in the right panel. The separating boundary defined by $\log_{10}(NPE) - 0.5 \cdot \mathcal{D} > 4$ is shown as black lines in the two dimensional plots.

the detector components deployed, may reach the sensitivity to probe current models of GZK neutrino fluxes.

## References


[1] K. Greisen, Phys. Rev. Lett. **16**, 748 (1966). G. T. Zatsepin and V. A. Kuzmin, Pisma Zh. Eksp. Teor. Fiz. **4**, 114 (1966) [JETP. Lett. **4**, 78 (1966)].

[2] R. Abbasi *et al.* (IceCube Collaboration), Nucl. Instrum. Meth. **A618**, 139 (2010).

[3] R. Abbasi *et al.* (IceCube Collaboration), Nucl. Instrum. Meth. **A601**, 294 (2009).

[4] M. Ackermann *et al.* (IceCube Collaboration), J. Geophys. Res. **111**, D13203 (2006).

[5] R. Abbasi *et al.* (IceCube Collaboration), Phys. Rev. **D82**, 072003 (2010).

[6] R. Abbasi *et al* (IceCube Collaboration), Phys. Rev. **D83**, 092003 (2011).

[7] S. Yoshida and M. Teshima, Prog. Theor. Phys. **89**, 833 (1993).

[8] R. Engel, D. Seckel, and T. Stanev, Phys. Rev. **D64**, 093010 (2001).

[9] E. Waxman and J. Bahcall, Phys. Rev. **D59**, 023002 (1999). S. Razzaque, P. Meszaros, and E. Waxman, Phys. Rev. **D68**, 083001 (2003).

[10] H. Johansson, PhD Thesis, Stockholm University, Sweden (2011).

[11] J. Abraham *et al.* (Pierre Auger Collaboration), Phys. Rev. **D79**, 102001 (2009).

[12] P. W. Gorham *et al.* (ANITA Collaboration), Phys. Rev. **D82**, 022004 (2010); arXiv:1011.5004 (erratum).

[13] D. Heck *et al.*, Report FZKA **6019** (Forschungszentrum Karlsruhe 1998).

[14] E. J. Ahn, R. Engel, T. K. Gaisser, P. Lipari, and T. Stanev, Phys. Rev. **D80**, 094003 (2009).

[15] R. Glasstetter *et al.*, Proc. 26th ICRC, Salt Lake City, USA (1999).

[16] S. Yoshida *et al.*, Phys. Rev. **D69**, 103004 (2004).

[17] J. Ahrens *et al.* (IceCube Collaboration), Nucl. Instrum. Meth. **A524**, 169 (2004).

[18] M. Honda *et al.*, Phys. Rev. **D75**, 043006 (2007).

[19] E. Bugaev *et al.*, Phys. Rev. **D58**, 054001 (1998).